JOURNAL OF CHEMICAL INFORMATION AND MODELING

Article

pubs.acs.org/jcim

Comparative Study on the Use of Docking and Bayesian Categorization To Predict Ligand Binding to Nicotinic Acetylcholine Receptors (nAChRs) Subtypes

David C. Kombo*,† and Merouane Bencherif

Targacept, Inc., 100 North Main Street, Winston-Salem, North Carolina 27101, United States

ABSTRACT: We have carried out a comparative study between docking into homology models and Bayesian categorization, as applied to virtual screening of nicotinic ligands for binding at various nAChRs subtypes (human and rat $\alpha4\beta2$, $\alpha7$, $\alpha3\beta4$, and $\alpha6\beta2\beta3$). We found that although results vary with receptor subtype, Bayesian categorization exhibits higher accuracy and enrichment than unconstrained docking into homology models. However, docking accuracy is improved when one sets up a hydrogen-bond (HB) constraint between the cationic center of the ligand and the main-chain carbonyl group of the conserved Trp-149 or its homologue (a residue involved in cation-π interactions with the ligand basic nitrogen atom). This finding suggests that this HB is a hallmark of nicotinic ligands binding to nAChRs. Best predictions using either docking or Bayesian were obtained with the human $\alpha7$ nAChR, when 100 nM was used as cutoff for biological activity. We also found that ligand-based Bayesian-derived enrichment factors and structure-based docking-derived enrichment factors highly correlate to each other. Moreover, they correlate with the mean molecular fractional polar surface area of actives ligands and the fractional hydrophobic/hydrophilic surface area of the binding site, respectively. This result is in agreement with the fact that hydrophobicity strongly contributes in promoting nicotinic ligands binding to their cognate nAChRs.

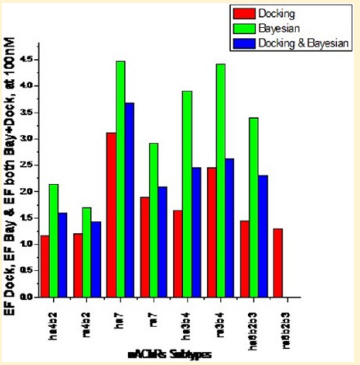

INTRODUCTION

nAChRs, also called NNRs (Neuronal Nicotinic Receptors), are pentameric membrane proteins that are members of the Cys-loop ligand-gated ion channel superfamily. Sixteen human genes encode for various nAChRs subunits which form homo- or heteropentamers with ubiquitous localization and are expressed differentially in various brain regions and throughout the human body. Receptors composed of $\alpha4$ and $\beta2$ subunits (the $\alpha4\beta2$* subtypes) and those containing $\alpha7$ subunits (the $\alpha7$* subtypes) represent the predominant populations of neuronal nAChRs in the Central Nervous System (CNS). These two receptors subtypes can have overlapping or complementing roles and participate broadly in various cognitive domains and attentional tasks (hippocampal and cortical through glutamate and acetylcholine modulation), in the regulation of sensory gating (P50, P300, mismatch negativity), in motoric functions in the nigro-striatal pathways (through regulation of dopaminergic neurons and cholinergic interneurons), and in addictive processes (mostly attributed to $\alpha4\beta2$* with a likely participation of $\alpha6$ and $\beta3$). Both the $\alpha4\beta2$* and the $\alpha7$* subtypes have been implicated in the regulation of fundamental pathways in neuroprotection and in the regulation of cytokine-mediated inflammation. Indeed the $\alpha7$* subtypes have been coined as the "central regulators of inflammation".[1]

Although it was long held that $\alpha7$ subunits form a homopentameric structure only, in addition to the dup-$\alpha7$ some evidence for coexpression with $\beta2$ eliciting modified function has been reported,[2,3] but their biological functions are unknown. In addition, receptors containing combinations of $\alpha2$, $\alpha3$, $\alpha5$, $\alpha6$, $\beta3$, or $\beta4$ subunits are also found in discrete CNS regions and could serve important physiological functions. Despite its predominant peripheral localization, the $\alpha3\beta4$* is expressed in discrete brain regions [e.g., nucleus tractus solitaris (NTS), the interpeduncular nucleus (IPN)] and can contribute to the function of the hypothalamo-pituitary axis and participate in peripheral physiological manifestations (e.g., emesis). In autonomic and sensory ganglia and in the adrenal gland, nAChRs containing the $\alpha3$ subunits in association with $\beta2$ and/or $\beta4$ subunits with or without the $\alpha5$ are predominant and mediate ganglionic transmission in sympathetic and parasympathetic systems.

nAChRs have been validated as drug targets for several CNS indications including schizophrenia, Parkinson's disease (PD), Alzheimer's disease (AD), and drug addiction.[4−7] Because of the heterogeneity of nicotinic receptors subtypes and their differing physiological roles, the optimization of the beneficial effects for indications such as AD, PD, or schizophrenia (e.g., $\alpha4\beta2$* and/or $\alpha7$*) must be accompanied by minimal interaction with receptors mediating gastrointestinal and cardiovascular side effects (e.g., $\alpha3\beta4$* receptors) or nicotinic receptors involved in biological processes not relevant to the target disease ($\alpha6\beta3$* in conditions where motoric or addictive processes are not or are only tangentially implicated in the etiopathogenesis of the targeted "disease"). Therefore,

Received: August 22, 2013
Published: November 28, 2013

predicting binding affinity to nAChRs is an important step toward designing better drugs against these protein targets.

Virtual screening is increasingly being used to find new compound hits, design *de novo* ligands, optimize lead compounds, and/or understand the potential mechanism(s) of action for various biological processes. The contribution of structure-based design (SBD) methods and ligand-based design (LBD) techniques in expediting early phases of the drug discovery cycle and reducing overall cost has been consistently demonstrated in modern pharmaceutical and biotechnology settings.[8] In recent years, numerous investigations about virtual screening have been extensively reported in the literature.[9−20] However, virtual screening success depends on many variables. Examples include the availability of the experimentally observed 3D structure of the protein target or the quality of the homology models used instead, the choice of the software version and its inherent options, the choice of actives and decoys, the choice of evaluation metrics, etc.

In a continuing effort to understand the molecular basis of the binding affinity and functional properties of nicotinic ligands toward their cognate nAChRs, we have recently reported various computational studies on their interactions with some nAChRs subtypes, using molecular docking,[21−29] pharmacophore modeling,[21,22,27,28] shape-based similarity,[26] and molecular descriptors calculations.[26,30] Numerous studies on virtual screening targeting nAChRs have also been reported by others in recent years.[31−41] Most of these studies have used molecular docking approach. In this paper, we focused on comparing docking into homology models derived for more nAChRs subtypes, and Bayesian categorization used to predict the binding of nicotinic ligands to these cognate receptors, using two definitions of actives and decoys, and two sets of docking options. We found that on the whole, Bayesian categorization exhibits higher accuracy and enrichment than unconstrained docking into homology models derived for nAChRs. However, setting up a HB constraint between the cationic center of the ligand and the main-chain carbonyl group of the highly conserved Trp-149 (or its homologue) can improve docking accuracy. Moreover, we found that Bayesian-derived enrichment factors (obtained from an LBD method) and docking-derived enrichment factors (obtained from an SBD approach) highly correlate to each other.

METHODS

Data Sets, Actives, and Decoys. nAChRs K_i data from our in-house compound collection were used as training, test, and validation sets. With the exception of rat $\alpha6\beta2\beta3$ K_i which was determined by autoradiography,[42] ligand displacement assay was used to determine the binding affinity for the $\alpha4\beta2$, $\alpha3\beta4$, and $\alpha7$ subtypes, as previously reported.[20−26] We have used two cutoffs to define actives. In one case, a compound is said to be an active binder to a given nAChR subtype, if $K_i \leq 100$ nM. A compound is categorized as a decoy if $K_i > 100$ nM. In the other case, a compound is considered an active binder to a given nAChR subtype, if $K_i \leq 500$ nM. Likewise, in this case, a compound is categorized as a decoy if $K_i > 500$ nM. Representative 2D structures of compounds used were previously exemplified and reported elsewhere.[21−30]

Comparative Modeling of nAChRs and Ligand Docking. Because the orthosteric binding site is in the extracellular region, homology models were developed for the extracellular domain of the pentameric human and rat protein targets $\alpha4\beta2$, $\alpha3\beta4$, $\alpha7$, and $\alpha6\beta2\beta3$, using the computer package Modeler,[43] as implemented within Discovery Studio (Accelrys, Inc., San Diego, CA, USA). In the case of the chimeric $\alpha6/\alpha3\beta2\beta3$ nAChRs, as the $\alpha3$-derived polypeptide chain which is added to an $\alpha6$ subunit to build the chimera is from the transmembrane domain,[44] it was not included in the homology modeling, as this was aimed at constructing the orthosteric binding site of the $\alpha6\beta2$ interface. The stochiometry used for both human and rat $\alpha4\beta2$, $\alpha3\beta4$, $\alpha7$, and $\alpha6\beta2\beta3$ nAChRs were $(\alpha4)_3(\beta2)_2$, $(\alpha3)_3(\beta4)_2$, $(\alpha7)_5$, and $(\alpha6\beta2)_2\beta3$, respectively. Model building, model validation, and ligand docking using the Glide software (Schrödinger, Inc., Portland, OR) were carried out following the procedures previously described.[21−29] In particular, a docking grid was constructed for each protein by using the centroid of the bound ligand and a maximum size of 20 Å. Flexibility of OH groups for amino acid side chains of Tyr, Ser, and Thr at the binding site was allowed. In one case, an H-bond constraint between the main chain CO group of a highly conserved TRP and the basic nitrogen of the ligand was specified, at the end of the docking run. In the other case, docking was carried out and analyzed without any constraint. During the stage of docking grid construction, Glide allows the user to set up constraints for receptor−ligand interactions that the user believes to be important to the binding mode, based on prior knowledge derived from structural or biochemical studies. In particular, an H-bond constraint is a requirement that a particular receptor−ligand hydrogen bond be made. The receptor atom must be a polar hydrogen, nitrogen, or oxygen atom. Limits on distances or angles between receptor and ligand atoms for the H-bond constraint are set internally by Glide as follows: H-acceptor distances of 1.2 to 2.5 Å; donor angles greater than 90°, and acceptor angles greater than 60°.

Bayesian Categorization Models. Bayesian models were derived using Pipeline Pilot (Accelrys, Inc., San Diego, CA). The following set of molecular descriptors was used: Functional class molecular fingerprints FCFP-6, LogD, molecular weight, (N + O) count, number of hydrogen-bond acceptor (HBA), number of hydrogen-bond donor (HBD), number of rotatable bonds, and molecular polar surface area. A two-way binning categorization approach was used for model building, with compounds considered to be "good" or active when K_i values were ≤100 nM (or 500 nM) and "bad" or inactive, otherwise. Models were validated using a Leave-One-Out cross-validation (XV-LOO) procedure and naïve test sets. In some cases, beside the test sets, performance evaluation of the models was further carried out using independent validation sets comprised of compounds which were synthesized and assayed a few months later, after the models were built.

Binding Site Hydrophobic/Hydrophilic Surface and Ligand Polarity. For each of the nAChRs subtypes studied herein, hydrophilic and hydrophobic surface areas were calculated using Maestro and dimeric interface of homology models, as previously described.[24,25] In the calculation, all residues located within a 6 Å distance to the highly conserved Trp residue located in the principal face of the protein binding site were included. Molecular fractional polar surface area of the ligand was computed using Pipeline Pilot (Accelrys, San Diego, CA, USA).

RESULTS

Predicted Binding Mode of Ligands at the Orthosteric Site of $(\alpha6\beta2)_2\beta3$ nAChR Subtype. We have recently reported on the predicted binding mode of nicotinic ligands at

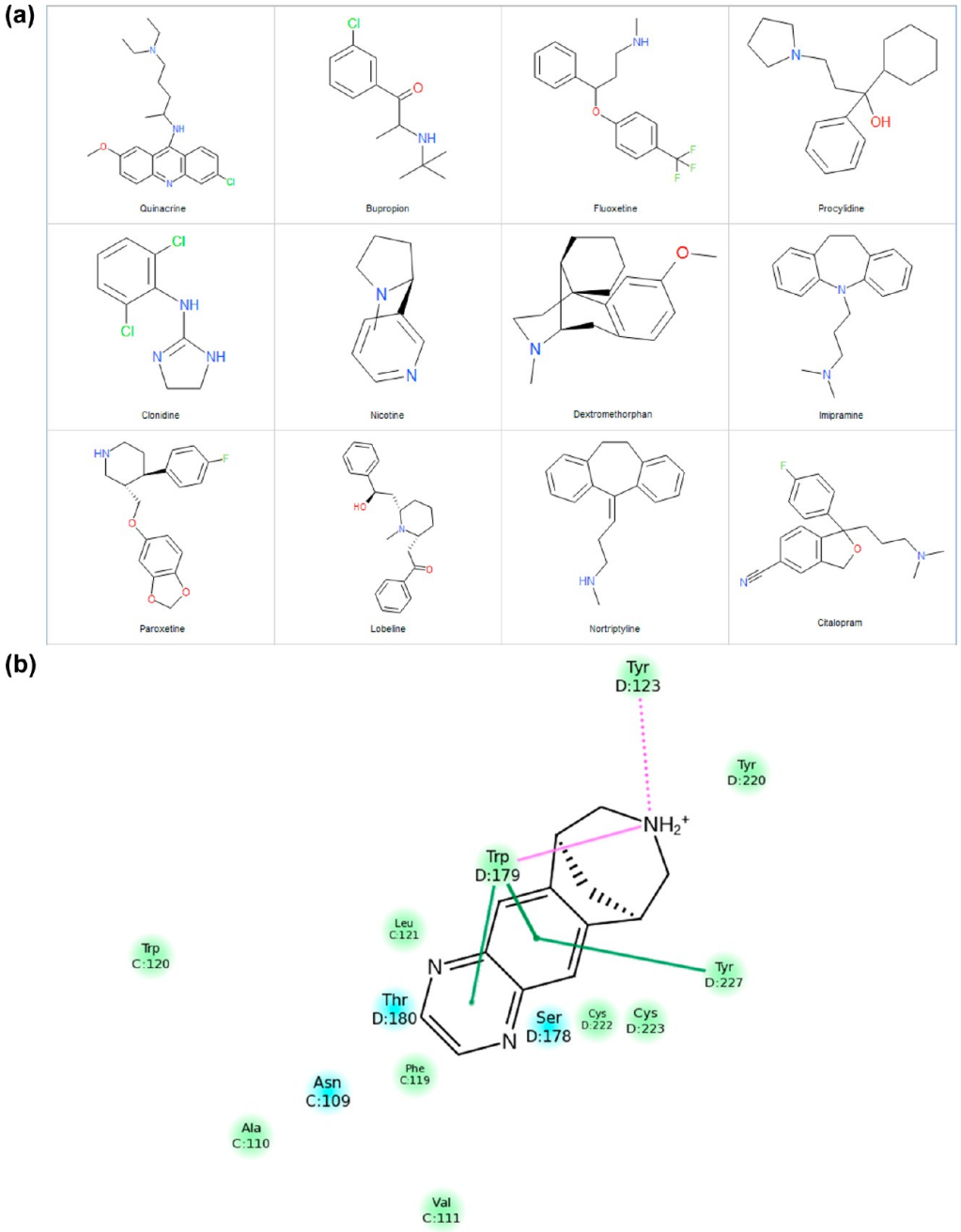

Figure 1. a. Exemplified structures of compounds used in this study. b. 2D interaction map diagram of the best pose obtained for Varenicline docked into human $\alpha6\beta2$* receptor. Hydrogen-bond interactions between the cation center of the ligand and the main chain carbonyl oxygen atom of the highly conserved Trp-179 and the side-chain hydroxyl oxygen atom of Tyr-123 are shown in magenta lines. Green lines indicate $\pi-\pi$ interactions between the ligand π rings and the aromatic side chain of Try-227 and Trp-179. Polar, hydrophobic, and charged amino acid residues located within a 5 Å distance from the ligand are highlighted in light blue, green, and purple, respectively.

the orthosteric binding site of $\alpha4\beta2$, $\alpha3\beta4$, and $\alpha7$ nAChRs subtypes as derived through docking into homology models.[21−29] We herein briefly describe the predicted binding mode of ligands at the orthosteric binding site of an $\alpha6$-containing nAChR subtype, namely the heteropentameric $(\alpha6\beta2)_2\beta3$ nAChR protein, derived by homology modeling, using the 3D structure of AChBP from the *Aplysia californica* species as a template (pdb code: 2byq). We chose this stoichiometry for modeling because concatameric $(\alpha6\beta2)_2\beta3$ nAChR protein has been demonstrated as fully functional.[42,44] Representative structures of compounds used herein are shown in Figure 1a. Moreover, additional structures used in this study have been already reported in our previous research articles.[21−30]

Test compounds were docked at the orthosteric binding site, located at the $\alpha6\beta2$ dimer interface. Figure 1b illustrates the binding mode of Varenicline, using a 2D interaction map representation. The cationic center of the ligand donates one hydrogen-bond to the backbone CO group of Trp-179, a highly conserved residue which is the homologue of the well-characterized Trp-149 located at the binding site of $\alpha4\beta2$ and $\alpha7$ nAChR subtypes. Varenicline is also involved in cation-π interactions and hydrophobic enclosures,[45,46] as shown in Figures 2a and 2b, respectively. Thus, similar to other nAChRs

dx.doi.org/10.1021/ci400493a | J. Chem. Inf. Model. 2013, 53, 3212−3222

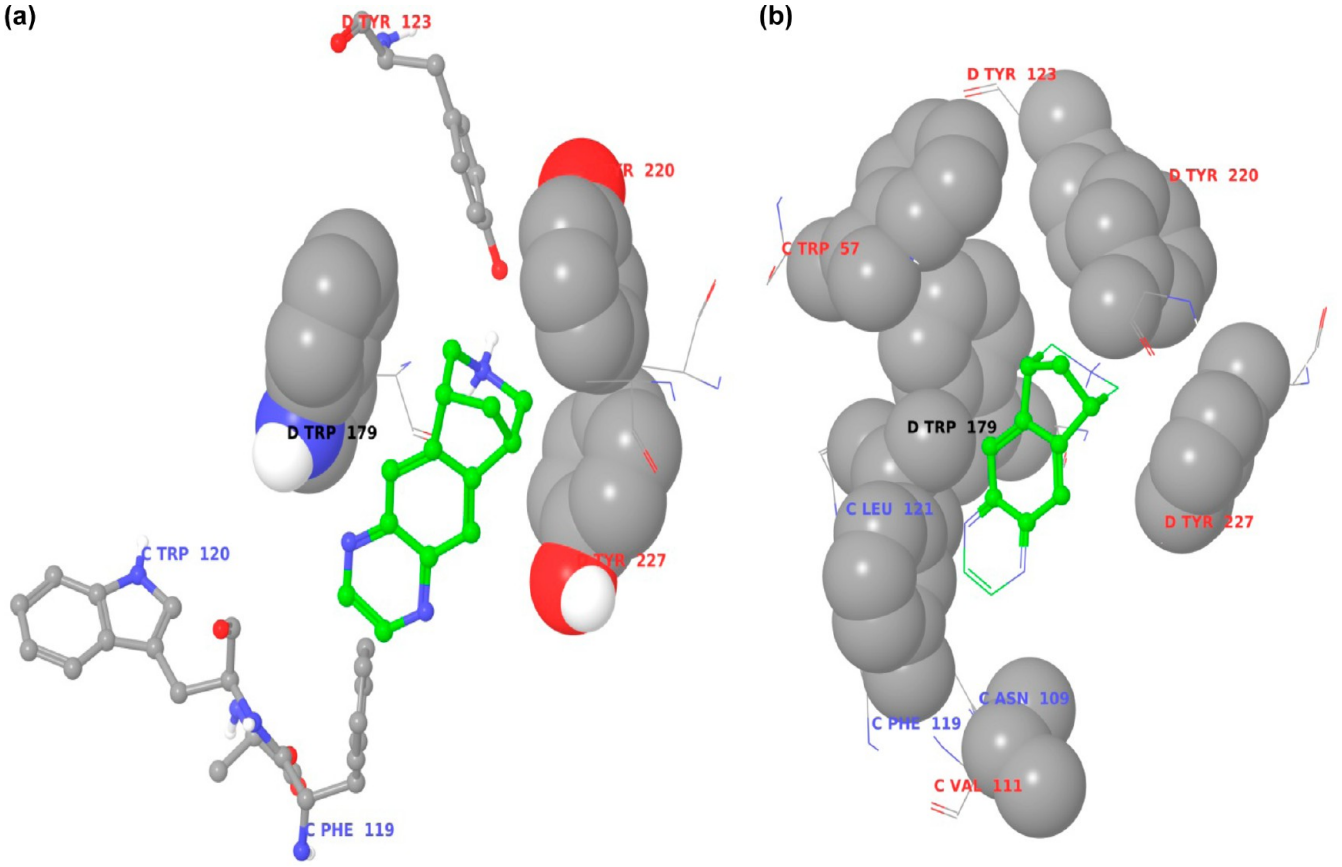

Figure 2. a. Best pose of varenicline docked into human $\alpha6\beta2$* homology model. The ligand is shown in ball and stick and colored green. Trp-179, Tyr220, and Tyr-227 (of the principal face), which are involved in cation-π interactions with the basic nitrogen of the ligand, are shown in space-filling representation. Also shown in ball and stick are Tyr-123, Phe-119, and Trp-120. b. Illustration of hydrophobic enclosures interactions encountered by varenicline in the orthosteric binding site of $\alpha6\beta2$. The best pose of varenicline docked into human $\alpha6\beta2$ homology model is shown in green. The moiety which is involved in hydrophobic enclosures interactions is illustrated in ball and thick stick, while the remaining of the ligand atoms are shown in thinner stick. The cognate amino acid residues which interact with the ligands are shown in space-filling representation.

Table 1. Training and Test Sets Accuracy Obtained for Bayesian Models Aimed at Predicting Binding Affinity to Various nAChRs Subtypes[a]

NNR		100 nM cutoff				500 nM cutoff		
	N	Accuracy Training	N	Accuracy Test	N	Accuracy Training	N	Accuracy Test
hα4β2	2048	0.92	3935	0.74	2048	0.93	3935	0.74
rα4β2	1139	0.87	3364	0.68	1139	0.91	3364	0.65
hα7	1650	0.85	2288	0.83	1650	0.86	2288	0.80
rα7	761	0.84	738	0.76	761	0.83	738	0.81
hα3β4	970	0.89	1428	0.80	970	0.86	1428	0.73
rα3β4	549	0.86	916	0.79	549	0.85	916	0.76
hα6β2β3	2211	0.94	1136	0.78	2211	0.90	1136	0.81
Average		0.88		0.77		0.88		0.76

[a]Accuracies ≥0.80 are highlighted in green, while accuracies ≥0.70 and <0.80 are highlighted in yellow. N designates the total number of compounds included in either the training or the test set.

dx.doi.org/10.1021/ci400493a | J. Chem. Inf. Model. 2013, 53, 3212−3222

Table 2. ROC Score Accuracy Obtained for Ligand Docking Aimed at Predicting Binding Affinity to Various nAChRs Subtypes[a]

NNR		100 nM cutoff				500 nM cutoff		
	N	(No Constr) Accuracy	N	(Constr) Accuracy	N	(No Constr) Accuracy	N	(Constr) Accuracy
hα4β2	3935	0.53	3935	0.76	3935	0.70	3935	0.87
rα4β2	3364	0.67	3364	0.76	3364	0.74	3364	0.90
hα7	2288	0.72	2288	0.83	2288	0.71	2288	0.82
rα7	738	0.66	738	0.73	738	0.64	738	0.76
hα3β4	1428	0.58	1428	0.65	1428	0.55	1428	0.63
rα3β4	916	0.66	916	0.74	916	0.69	916	0.70
hα6β2β3	1136	0.67	1136	0.74	1136	0.67	1136	0.76
rα6β2β3	55	0.54	55	0.79	55	0.54	55	0.79
Average		0.63		0.74		0.66		0.78

[a]Accuracies ≥0.80 are highlighted in green, while accuracies ≥0.70 and <0.80 are highlighted in yellow. N designates the total number of compounds docked in each case. The docked data set is identical to the one used as the test set for the Bayesian models, as shown in Table 1.

subtypes, ligand-$\alpha6\beta2\beta3$ receptor recognition process is mediated primarily through hydrogen-bond, $\pi-\pi$, cation-π, hydrophobic enclosures, and pairwise lipophilic interactions. A detail analysis of docking poses obtained for ligand-$\alpha6\beta2\beta3$ nAChR interactions, in the case of TC-8831, a compound efficacious in alleviating L-dopa induced dyskinesia,[42,47,48] will be reported in a full structure−activity relationship (SAR) paper elsewhere.

ROC Score-Derived Accuracy of Bayesian Models Aimed at Predicting Nicotinic Ligand Binding. To evaluate the accuracy of the predictive model, we have determined the receiver operating characteristic curve (ROC) score, which provides a simple quality assessment for a classification model. It is a number between 0.5 and 1.0. The closer the ROC score is to 1.0, the better the model is at distinguishing active (good) from inactive (bad) samples. Results shown in Table 1 indicate that Bayesian models provide good accuracy for most K_i end points. When the 100 nM cutoff is used, Table 1 indicates that the accuracy obtained for the training set varies within the range 0.84−0.94, whereas the corresponding test set accuracy varies within the range 0.68−0.83. When the 500 nM cutoff is used, Table 1 indicates that the accuracy obtained for the training set varies within the range 0.83−0.93, whereas the corresponding test set accuracy varies within the range 0.65−0.81. Results shown at the bottom of Table 1 suggest that the training set accuracy obtained at both cutoffs is the same (an average of 0.88 in both cases). Likewise, the accuracies obtained at both cutoffs for the test sets are almost identical (averages of 0.77 and 0.76). We also find that at both cutoffs, only the models aimed at predicting ligand binding to human $\alpha7$ nAChR subtype exhibits an accuracy ≥0.80, and only the models aimed at predicting ligand binding to rat $\alpha4\beta2$ nAChR subtype exhibits an accuracy <0.70. Due to a limited data set for rat $\alpha6\beta2\beta3$, Bayesian models were not built for this subtype.

ROC Score-Derived Accuracy of Docking Models Aimed at Predicting Nicotinic Ligand Binding. Table 2 shows the ROC score accuracy derived when the same compounds used as test set to evaluate the performance of Bayesian models (see Table 1) were docked into corresponding homology models. Results indicate that on the whole, docking models provide good accuracy only when HB constraints are used. When the 100 nM cutoff is used, Table 2 indicates that the constrained docking accuracy obtained varies within the range 0.65−0.83, whereas the corresponding unconstrained docking accuracy varies within the range 0.53−0.72. When the 500 nM cutoff is used, Table 2 indicates that the constrained docking accuracy varies within the range 0.63−0.90, whereas the corresponding unconstrained docking accuracy varies within the range 0.54−0.74. Average scores shown at the bottom of Table 2 suggest that setting up the HB constraint increases docking accuracy for both cutoffs used (0.74 vs. 0.63 at 100 nM cutoff and 0.78 vs 0.66 at 500 nM cutoff). We also find that at 100 nM cutoff, ligand docking into human $\alpha7$ nAChR subtype exhibits the highest accuracy, both in the presence and absence of the HB constraint. Moreover, at 500 nM cutoff, docking into human $\alpha7$, human $\alpha4\beta2$, and rat $\alpha4\beta2$ nAChRs subtypes exhibit the 3 highest accuracies, both in the presence and absence of the HB constraint. To further confirmed the trend in docking accuracy observed herein, we derived the average number of outranking decoys. Results shown in Figure 3a indeed suggest that the number of false positives as expressed in terms of average number of outranking decoys increase when the HB constraint is removed, in the case of actives @ 100 nM cutoff, thereby lowering docking accuracy. A similar result is obtained when a 500 nM cutoff is used, as shown in Figure 3b.

Enrichment Factors Computed for Both Docking and Bayesian Models. In addition to evaluating the accuracy of the predictive models by computing the ROC score, we have estimated enrichment factors (EF). An enrichment plot shows how well the model assigns higher scores to known active compounds, than to known decoys. EF@10% is calculated as follows:

dx.doi.org/10.1021/ci400493a | J. Chem. Inf. Model. 2013, 53, 3212−3222

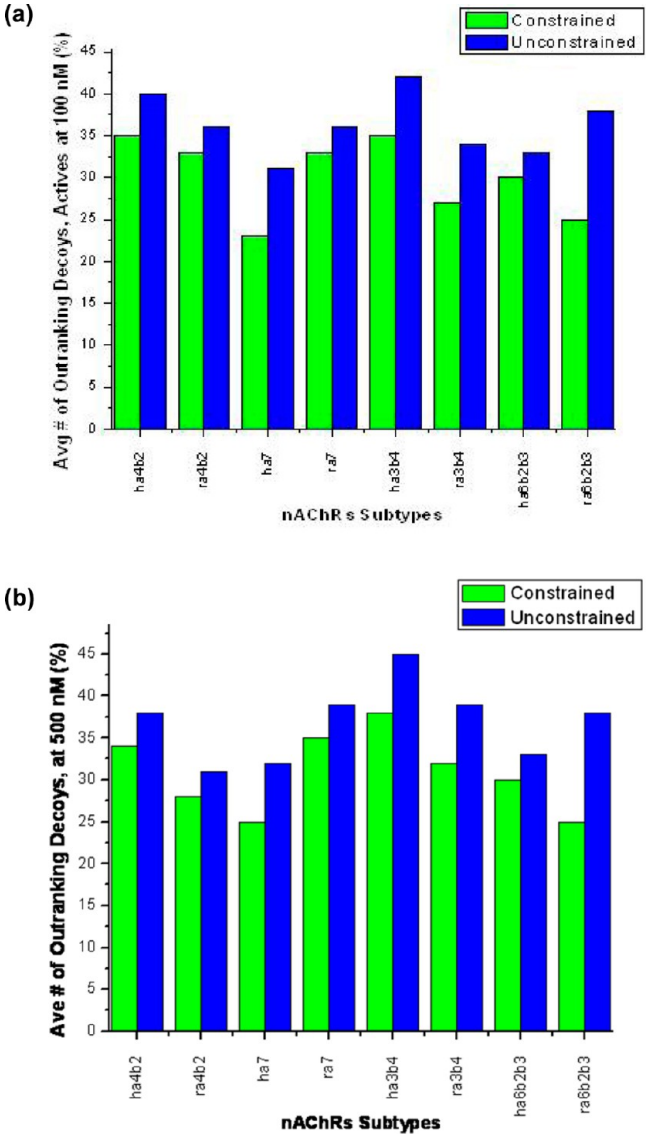

Figure 3. a. Average number of outranking decoys obtained for constrained vs unconstrained docking, using a 100 nM cutoff for biological activity. b. Average number of outranking decoys obtained for constrained vs unconstrained docking, using a 500 nM cutoff for biological activity.

$$\text{EF@10\%} = (\text{TP@10\% of sorted hit list}) / (\text{total number of actives}) \quad (1)$$

where (TP@10% of sorted hit list) designates the total number of true positives recovered at the top 10% of the sorted hit list. One should note that the higher the EF, the better the model can be used to screen a database. Results shown in Table 3 indicate that Bayesian models consistently exhibit higher enrichment factors than docking with constraints. Combining both Bayesian and docking screening slightly increase enrichment factor in comparison to performing docking alone: EF Dock < EF Bay and Dock < EF Bay. Table 3 also shows that the highest enrichment factor EF@10% is obtained with the human $\alpha 7$ nAChR, for both docking and Bayesian categorization, using either 100 nM or 500 nM as cutoff.

Table 4 shows results obtained with a validation set made of diverse compounds synthesized and assayed against three receptors subtypes, after the Bayesian models were built and

Table 3. (EF@10%) Computed for Both Bayesian Models and Constrained Docking

NNR		100 nM cutoff				500 nM cutoff		
	N Actives	EF Dock	EF Bay	EF Both	N Actives	EF Dock	EF Bay	EF Both
hα4β2	1699	1.17	2.14	1.60	2434	1.15	1.55	1.33
rα4β2	1741	1.20	1.70	1.43	2352	1.19	1.36	1.27
hα7	219	3.11	4.47	3.67	415	2.63	3.45	2.86
rα7	175	1.89	2.91	2.09	324	1.54	2.16	1.70
hα3β4	218	1.65	3.90	2.45	479	1.23	2.51	1.75
rα3β4	102	2.45	4.41	2.62	258	1.82	2.60	1.88
hα6β2β3	180	1.44	3.39	2.31	352	1.45	2.56	1.95
rα6β2β3	46	1.30			47	1.28		
Average		1.78	3.27	2.31		1.54	2.31	1.82

initial docking was carried out. We find that both at 100 nM and 500 nM cutoffs, Bayesian models aimed at predicting ligand binding at human $\alpha 4\beta 2$, rat $\alpha 4\beta 2$, and human $\alpha 6\beta 2\beta 3$ nAChRs subtypes exhibit a higher EF@10% than constrained docking. However, the accuracy of the model appears to be higher for constrained docking as compared to Bayesian models, as previously observed with the test set for both human $\alpha 4\beta 2$ and rat $\alpha 4\beta 2$ nAChR subtypes (see Tables 1 and 2).

Bayesian-Derived Enrichment Factors Correlate with Docking-Derived Enrichment Factors. Figure 4a shows that Bayesian EF@10% correlates with docking EF@10%. A linear equation relates them with an $r^2 = 0.67$ and a regression p-value = 0.024, when a 100 nM cutoff is used for biological activity. A higher correlation with $r^2 = 0.71$ and a regression p-value = 0.017 is even observed when a 500 nM cutoff is used for biological activity, as shown in Figure 4b.

In addition to correlating with Bayesian-derived EF@10%, docking-derived EF@10% correlates with the ratio of the binding site hydrophobic molecular surface area to the binding site hydrophilic molecular surface area. We have coined this ratio as "binding site fractional hydrophobic surface area". The values of r^2 parameter obtained for this correlation when using a cutoff of 100 nM and 500 nM were 0.76 and 0.74, respectively. Results are shown in Figures 5a and 5b. Similarly, Bayesian-derived EF@10% inversely correlates with the mean molecular fractional polar surface area of actives ligands for each nAChR subtype. The values of r^2 parameter obtained for this correlation when using a cutoff of 100 nM and 500 nM were 0.77 and 0.79, respectively. Results are shown in Figures 6a and 6b.

DISCUSSION

We have found that on the whole, Bayesian categorization appears to be more accurate than unconstrained docking in predicting nicotinic ligand binding to their nAChRs cognates, as shown in Tables 1 and 2. A student t test showed that the accuracy of Bayesian models and the accuracy obtained for unconstrained docking at 100 nM and 500 nM cutoffs are statistically significantly different, with p-values of 0.0016 and 0.03, respectively. However, setting a HB constraint involving the main-chain CO group of the conserved Trp-149 (or its

dx.doi.org/10.1021/ci400493a | J. Chem. Inf. Model. 2013, 53, 3212−3222

Table 4. Accuracy and Enrichment Factor of Bayesian and Constrained Docking Models for Validation Sets Synthesized and Assayed within 4 Months after Model Building Studies[a]

NNR		100 nM Cutoff				500 nM Cutoff			
	N	Accuracy Bayesian	Accuracy Docking	EF@10% Bayesian	EF@10% Docking	Accuracy Bayesian	Accuracy Docking	EF@10% Bayesian	EF@10% Docking
hα4β2	243	0.68	0.88	4.10	2.0	0.75	0.78	1.30	1.20
r α4β2	75	0.70	0.78	1.82	1.59	0.53	0.56	1.08	1.08
hα6β2β3	261	0.87	0.94	8.75	4.40	0.80	0.94	7.50	4.50
Average		0.75	0.87	4.89	2.66	0.69	0.76	3.29	2.26

[a]Accuracies ≥0.80 are highlighted in green, while accuracies ≥0.70 and <0.80 are highlighted in yellow. N designates the total number of compounds docked in each case. The docked data set is identical to the one used to validation the Bayesian models.

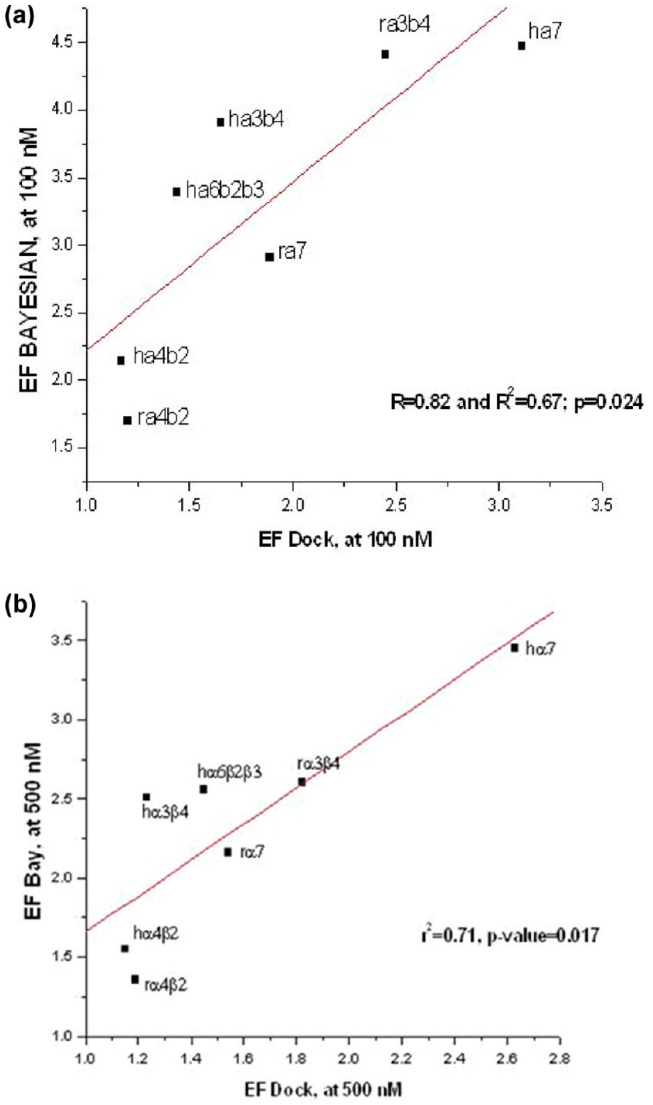

Figure 4. a. Bayesian-derived EF@10% plotted vs docking-derived EF@10%. 100 nM was used as cutoff for biological activity, for each of the nAChRs subtypes studied herein. b. Bayesian-derived EF@10% plotted vs docking-derived EF@10%. 500 nM was used as cutoff for biological activity, for each of the nAChRs subtypes studied herein.

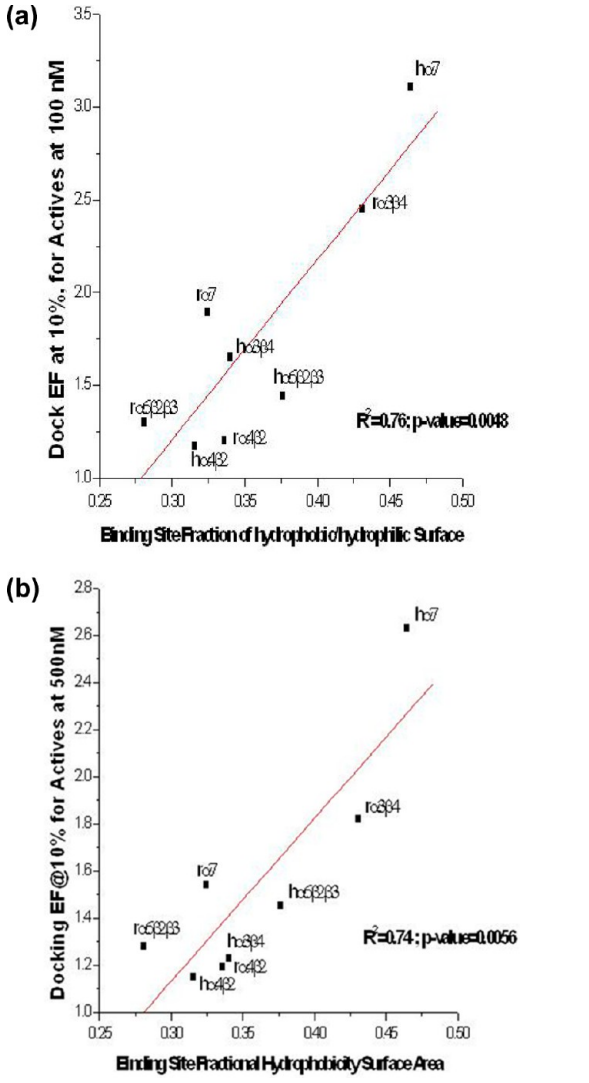

Figure 5. a. Docking-derived EF@10% plotted vs binding site fractional hydrophobic surface area. 100 nM was used as cutoff for biological activity, for each of the nAChRs subtypes studied herein. b. Docking-derived EF@10% plotted vs binding site fractional hydrophobic surface area. 500 nM was used as cutoff for biological activity, for each of the nAChRs subtypes studied herein.

homologue residue) of the principal face improves docking accuracy until it almost equals the results obtained with Bayesian categorization, as also shown in Tables 1 and 2. A student *t* test showed that the accuracy of Bayesian models and the accuracy obtained for constrained docking at 100 nM and 500 nM cutoffs are not statistically significantly different, with p-values of 0.20 and 0.34, respectively. In some cases such as the ones shown in Table 4, HB-constrained docking appears to be more accurate than Bayesian categorization. On the whole, these results suggest that this HB, which was originally observed by Dougherty and co-workers in their studies of nicotine interacting with $\alpha4\beta2$ nAChR,[49] is a hallmark of nicotinic ligand binding to nAChRs. Besides the ROC score obtained, the average number of outranking decoys, as shown in Figure 3, also corroborates the improvement in accuracy

dx.doi.org/10.1021/ci400493a | J. Chem. Inf. Model. 2013, 53, 3212−3222

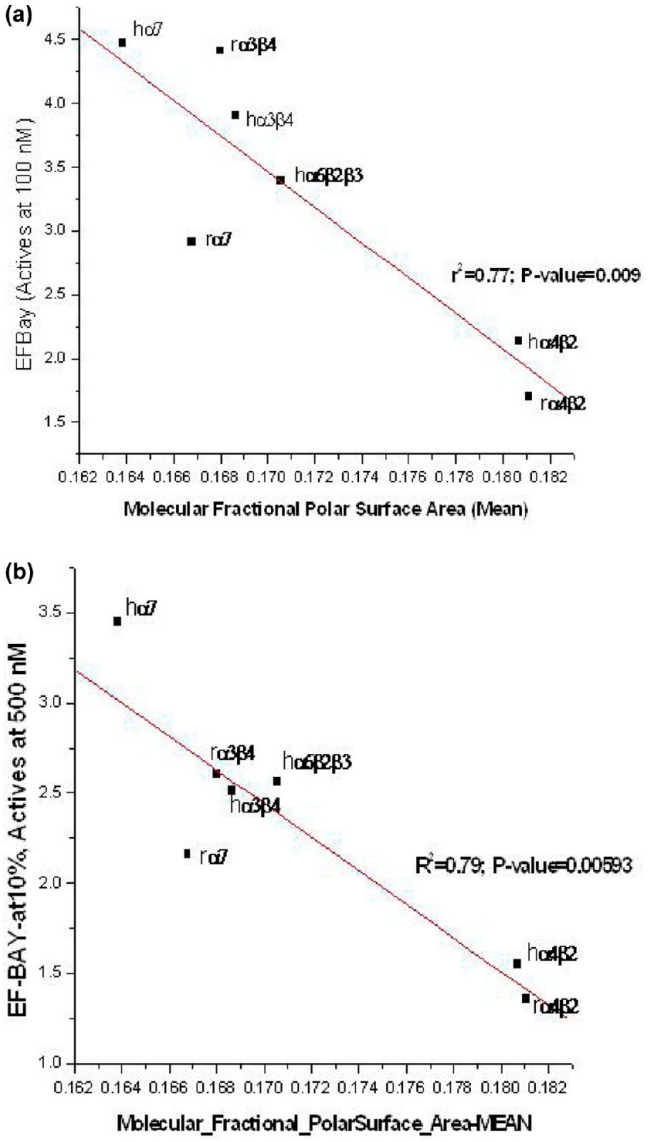

Figure 6. a. Bayesian-derived EF@10% plotted vs mean molecular fractional polar surface of active compounds, when 100 nM was used as cutoff for biological activity, for each of the nAChRs subtypes studied herein. b. Bayesian-derived EF@10% plotted vs mean molecular fractional polar surface of active compounds when 500 nM was used as cutoff for biological activity, for each of the nAChRs subtypes studied herein.

upon introducing a docking constraint requirement, as the average number of false positives decrease. When comparing all the nAChRs subtypes, we found that best predictions, when using either docking or Bayesian methods with a 100 nM cutoff for biological activity, were obtained with human α7 nAChR. However, a similar result is not observed with its most closely related rat α7 nAChR subtype. This suggests that nicotinic ligands may present significant differences when binding to the human vs rat α7 nAChR subtypes, due to the existence of multiple interaction regions and alternative binding modes at the binding site of these two proteins, as previously reported.[21,22,50]

We have found that Bayesian categorization exhibits higher enrichment factor @10% than docking into homology models, to predict binding to nAChRs, as shown in Tables 3 and 4. A student *t* test showed that EF@10% of Bayesian models and constrained docking at 100 nM and 500 nM cutoffs are statistically significantly different, with p-values of 0.0005 and 0.001, respectively. One should note that it has been previously reported that other ligand-based methods such as 2D ligand similarity and 3D ligand similarity exhibit better enrichment factors than ligand docking into crystal structures of diverse receptors different from nAChRs.[20] However, EF@10% obtained for constrained docking can be improved when both Bayesian and docking methods are used in conjunction, as they appear to be complementary (Table 3).

Our studies have also shown that Bayesian EF@10% linearly correlates with docking EF@10%, as shown in Figures 4a and 4b. The r^2 values obtained at 100 nM and 500 nM cutoffs were 0.67 and 0.71, respectively, with linear regression p-values of 0.024 and 0.017, respectively. It is noteworthy remembering that both the structure-based docking and ligand-based Bayesian categorization procedures used herein neglect the contribution of receptor flexibility. In future studies, it would be interesting to see how results derived from induced-fit docking studies would compare with results obtained from Bayesian categorization or other ligand-based techniques such as recursive partitioning, K-nearest neighbors, etc.

Furthermore, as shown in Figures 5a and 5b, we have also found that docking-derived EF@10% strongly correlates with binding site fractional hydrophobic surface area. The latter term has been first introduced herein and defined as the ratio of binding site hydrophobic molecular surface area to the hydrophilic molecular surface area. Similarly, Bayesian-derived EF@10% inversely correlates with the mean value of molecular fractional polar surface area of actives ligands at each nAChR subtype, as shown in Figures 6a and 6b. These findings are in agreement with the contribution of a hydrophobic moiety in the molecular recognition process of ligand binding at the orthosteric site of nAChRs, as highlighted by the well-known nicotinic pharmacophore. Descriptors used in building Bayesian models include bulk properties such as LogD and molecular polar surface area. This does not favor Bayesian models over docking, as the latter also estimate pairwise lipophilic interactions and hydrophobic enclosures as well. Moreover, results obtained from calculations of binding site fractional hydrophobic surface area (Figure 5b) suggest the following decreasing order of hydrophobicity for nAChRs: hα7 > rα3b4 > h$\alpha6\beta2\beta3$ > h$\alpha3\beta4$ > r$\alpha4\beta2$ > rα7 > h$\alpha4\beta2$ > r$\alpha6\beta2\beta3$. These results are in agreement with our previous data on binding site hydrophilic surface area of various nAChRs which we found to correlate with free energy of binding of the marine toxins 13-desmethylspirolide C and gymnodimine.[24] Because the Bayesian-derived enrichment factor is directly proportional to docking-derived enrichment factor, as shown in Figure 4b, it appears that docking does not do better in the receptors less dependent on hydrophobicity (e.g., rα7, h$\alpha4\beta2$, and r$\alpha6\beta2\beta3$) for structure−activity relationships.

Both the training and test sets were randomly selected from the population of available compounds tested. However, our findings that Bayesian models exhibit higher enrichment factor than docking are based on 7 different subtypes, both human and rat subtypes, thus reducing the randomness element. The test sets used at the construction of the Bayesian models contain the most valuable information for the following 2 reasons. First, they were much larger than the ones derived from later synthesized compounds. Second, they came from 7 different nAChR subtypes, whereas the test sets derived from later synthesized compounds came from a limited data set

made of 3 subtypes only. Depending on the drug development stage and the availability of data sets, enrichment factor metrics can be most important than overall accuracy and vice versa. At the beginning of a lead identification stage, where the size of the available SAR data sets is not big enough to build and validate a decent Bayesian model, docking using a crystal structure or a 3D model derived by homology modeling can be most valuable. However, with the increase of publically available databases containing binding affinity on the Internet, one can still find enough data to build Bayesian models at the beginning of the project. If not, with the increase of the data set size as it happens in a lead optimization stage, it readily becomes possible to build and validate accurate Bayesian models. These can then be used to screen new virtual libraries suggested by both medicinal chemists and computational chemists. The higher the enrichment factor, the smaller the number of compounds will be synthesized in order to obtain some actives compounds, thereby reducing operational cost. Likewise, with higher enrichment factors, Bayesian models can be very useful when screening external vendor databases in an attempt to diversify and enrich a corporate database. In a lead optimization stage, compounds synthesized latter are usually least like the data set that one starts with at the beginning. The finding that Bayesian models still exhibit higher enrichment factors even with a later synthesized test set suggests that its performance is data set independent, thereby adding value to the importance of this simple and fast method as a virtual screening tool.

The limitation observed with unconstrained docking using the force field-based Glide software in modeling ligand-nAChRs interactions is likely due to the fact that at the current stage of force field formalism, cation-π interactions are not well taken into account. Glide SP, the level of theory at which our studies were carried out, completely neglects them. However, Glide XP attempts to approximately include their contributions by using rewards for cation$-\pi$ interactions. These are favorable energetic contributions to the binding affinity resulting from cation-π interactions, as assigned and calculated within the Glide XP scoring scheme. It is well-known that cation-π interactions between the basic nitrogen and the highly conserved Trp-149 strongly contribute to nicotinic ligands binding free energy and are accompanied by hydrogen-bond interaction between the cationic center and the main-chain carbonyl oxygen atom of Trp-149.[49] Setting up a HB constraint may thus be an indirect way of attempting to compensate for one of the missing important dual interactions. It is worth mentioning that using an equivalent HB constraint when docking ligands into the homologous pentameric 5HT-3A serotogenic receptor, which also involve strong cation-π interactions, we were able to explain the selectivity of TC-5619 for a7 nAChR over its serotogenic counterpart.[25]

To further determine statistical significance of the results obtained for the accuracy tests, we performed a student t test. Results indicate that the values of accuracy obtained when docking with constraint vs unconstrained docking using either 100 nM or 500 nM cutoffs are indeed statistically significant, with p-values of 0.0004 and 0.0003, respectively. Student t test results also indicate that the accuracies obtained when docking with constraints using a 100 nM cutoff for biological activity are not significantly different from the ones obtained when docking with constraints using a 500 nM cutoff for biological activity, with a p-value of 0.12. Likewise, the Bayesian-derived accuracies when using a 100 nM cutoff for biological activity are not statistically significant from the Bayesian-derived accuracies when one uses a 500 nM cutoff for biological activity, with a p-value of 0.24.

CONCLUSION

Our aims and objectives were to compare an LBD method, namely Bayesian categorization, to an SBD method, namely docking into homology models, to predict ligand binding to nAChRs. The ultimate goal was to determine which method is best for virtual screening prior to synthesis and database mining, in the nicotinic drug discovery landscape. For the SBD method, we have also assessed both the utility of a HB constraint and the sensitivity for various nAChRs subtypes toward hydrophobic/hydrophobic surface area at the binding site. For the LBD method, we have assessed the sensitivity for various nAChRs subtypes toward ligand hydrophobicity/polarity. We have found that Bayesian categorization exhibits higher Enrichment Factor @10% than docking into homology models, to predict binding to nAChRs. Docking-derived EF@10% can be improved, however, when both SBD and LBD methods are considered, as they appear to be complementary. Best predictions using either docking or Bayesian were obtained with human α7 nAChRs, when the cutoff for biological activity was set to 100 nM K_i, thus including only tightest binders. We have also found that setting a HB constraint involving the main-chain carbonyl group of the conserved Trp-149 of the principal face improves docking accuracy, suggesting that this HB is a hallmark of ligand binding to nAChRs. Bayesian-derived EF@10% highly correlates with docking EF@10% which in turn directly correlates with binding site fractional hydrophobic surface area. Furthermore, Bayesian-derived EF@10% inversely correlates with the mean of molecular fractional polar surface area of actives ligands at each nAChR subtype. These unexpected and encouraging findings can be exploited to design better nicotinic drugs to tackle various CNS disorders.

AUTHOR INFORMATION

Corresponding Author

*E-mail: dckombo777@mail.com.

Present Address

[†]Proteostasis Therapeutics Inc., 200 Technology Square, Cambridge, MA 02139.

Notes

The authors declare no competing financial interest.

ACKNOWLEDGMENTS

We thank Dr. Jason Speake and the whole Medicinal Chemistry team under his supervision, for making most of compounds studied herein. We thank Terry Hauser and the whole Neurochemistry group under his leadership, for their contributions in developing and performing the nAChR binding assays. We also thank Dr. Phil Hammond and Mauri Hodges for helpful discussions and support, respectively.

ABBREVIATIONS USED:

ACHBP, acetylcholine-binding protein; Ach, acetylcholine; CNS, central nervous system; nAChR, nicotinic acetylcholine receptor; NNR, neuronal nicotinic receptor; Pdb, protein databank; rmsd, root-mean-squared-deviation; SP, standard precision; XP, extra precision; EF, enrichment facor; Roc score, receiver operating characteristic curve; LBD, ligand-based design; SBD, structure-based design; PD, Parkinson's disease;

AD, Alzheimer's disease; NTS, nucleus tractus solitaris; IPN, interpeduncular nucleus; HBA, number of hydrogen-bond acceptors; HBD, number of hydrogen-bond donors; SAR, structure−activity relationship

REFERENCES

(1) Wang, H.; Yu, M.; Ochani, M.; Amella, C. A.; Tanovic, M.; Susarla, S.; Li, J. H.; Wang, H.; Yang, H.; Ulloa, L.; Al-Abed, Y.; Czura, C. J.; Tracey, K. J. Nicotinic acetylcholine receptor alpha7 subunit is an essential regulator of inflammation. *Nature* **2003**, *421*, 384−388.

(2) Liu, Q.; Huang, Y.; Xue, F.; Simard, A.; DeChon, J.; Li, G.; Zhang, J.; Lucero, L.; Wang, M.; Sierks, M.; Hu, G.; Chang, Y.; Lukas, R. J.; Wu, J. J. A novel nicotinic acetylcholine receptor subtype in basal forebrain cholinergic neurons with high sensitivity to amyloid peptides. *J. Neurosci.* **2009**, *29*, 918−929.

(3) Liu, Q.; Huang, Y.; Shen, J.; Steffensen, S.; Wu, J. Functional $\alpha7\beta2$ nicotinic acetylcholine receptors expressed in hippocampal interneurons exhibit high sensitivity to pathological level of amyloid β peptides. *BMC Neurosci.* **2012**, *13*, 155.

(4) Philip, N. S.; Carpenter, L. L.; Tyrka, A. R.; Price, L. H. The nicotinic acetylcholine receptor as a target for antidepressant drug development. *Psychopharmacology (Berlin, Ger.)* **2011**, *212*, 1.

(5) Taly, A.; Corringer, P. J.; Guedin, D.; Lestage, P.; Changeux, J. P. Nicotinic receptors: allosteric transitions and therapeutic targets in the nervous system. *Nat. Rev. Drug Discovery* **2009**, *8*, 733−750.

(6) Lippiello, P. M.; Bencherif, M.; Hauser, T. A.; Jordan, K. G.; Letchworth, S. R.; Mazurov, A. A. Nicotinic receptors as targets for therapeutic discovery. *Expert Opin. Drug Discovery* **2007**, *2*, 1185−1203.

(7) Romanelli, M. N.; Gratteri, P.; Guangalini, L.; Martini, E.; Bonaccini, C.; Gualtieri, F. Central nicotinic receptors: structure, function, ligands, and therapeutic potential. *ChemMedChem* **2007**, *2*, 746−767.

(8) Leach, A. R. *Molecular modeling principles and applications*, 2nd ed.; Prentice Hall: New Jersey, USA, 2001.

(9) Hassan, M.; Brown, R. D.; Varma-O'Brien, S.; Rogers, D. Cheminformatics analysis and learning in a data pipelining environment. *Mol. Diversity* **2006**, *10*, 283−299.

(10) Lee, P. H.; Cucurull-Sanchez, L.; Lu, J.; Du, Y. J. Development of in silico models for human liver microsomal stability. *J. Comput.-Aided Mol. Des.* **2007**, *21*, 665−673.

(11) Vogt, M.; Bajorath, J. Bayesian screening for active compounds in high-dimensional chemical spaces combining property descriptors and molecular fingerprints. *Chem. Biol. Drug Des.* **2008**, *71*, 8−14.

(12) Venhorst, J.; Nunez, S.; Terpstra, J. W.; Kruse, C. G. Assessment of scaffold hopping efficiency by use of molecular interaction fingerprints. *J. Med. Chem.* **2008**, *51*, 3222−3229.

(13) Cannon, E. O.; Bender, A.; Palmer, D. S.; Mitchell, J. B. Chemoinformatics-based classification of prohibited substances employed for doping in sport. *J. Chem. Inf. Model.* **2006**, *46*, 2369−2380.

(14) Huang, D.; Gu, Q.; Ge, H.; Ye, J.; Salam, N. K.; Hagler, A.; Chen, H.; Xu, J. On the value of homology models for virtual screening: discovering hCXCR3 antagonists by pharmacophore-based and structure-based approaches. *J. Chem. Inf. Model.* **2012**, *52*, 1356−1366.

(15) Pitt, W. R.; Calmiano, M. D.; Kroeplien, B.; Taylor, R. D.; Turner, J. P.; King, M. A. Structure-based virtual screening for novel ligands. *Methods Mol. Biol.* **2013**, *1008*, 501−519.

(16) Sakkiah, S.; Arullaperumal, V.; Hwang, S.; Lee, K. W. Ligand-based pharmacophore modeling and Bayesian approaches to identify c-Src inhibitors. *J. Enzyme Inhib. Med. Chem.* **2013**, Feb25 [Epub ahead of print].

(17) Lill, M. Virtual screening in drug design. *Methods Mol. Biol.* **2013**, *993*, 1−12.

(18) Jain, A. N. Virtual screening in lead discovery and optimization. *Curr. Opin. Drug Discovery Dev.* **2004**, *7*, 396−403.

(19) Zoete, V.; Grosdidier, A. Docking, virtual high throughput screening and in silico fragment-based drug design. *J. Cell. Mol. Med.* **2009**, *13*, 238−248.

(20) McGaughey, G. B.; Sheridan, R. P.; Bayly, C. I.; Culberson, J. C.; Kreatsoulas, C.; Lindsley, S.; Majorov, V.; Truchon, J. F.; Cornell, W. D. Comparison of topological, shape, and docking methods in virtual screening. *J. Chem. Inf. Model.* **2007**, *47*, 1504−1519.

(21) Kombo, D. C.; Mazurov, A. A.; Tallapragada, K.; Hammond, P. S.; Chewning, J.; Hauser, T. A.; Vasquez-Valdivieso, M.; Yohannes, D.; Talley, T. T.; Taylor, P.; Caldwell, W. S. Docking studies of benzylidene anabaseine interactions with $\alpha7$ nicotinic acetylcholine receptor (nAChR) and acetylcholine binding proteins (AChBPs): application to the design of related $\alpha7$ selective ligands. *Eur. J. Med. Chem.* **2011**, *46*, 5625−5635.

(22) Kombo, D. C.; Mazurov, A. A.; Tallapragada, K.; Hammond, P. S.; Chewning, J.; Hauser, T. A.; Speake, J.; Yohannes, D.; Caldwell, W. S. Discovery of novel $\alpha7$ nicotinic acetylcholine receptor ligands via pharmacophoric and docking studies of benzylidene anabaseine analogs. *Bioorg. Med. Chem. Lett.* **2012**, *22*, 1179−1186.

(23) Kombo, D. C.; Hauser, T. A.; Grinevich, V. P.; Melvin, M. S.; Strachan, J.-P.; Sidach, S. S.; Chewning, J.; Hammond, P. S.; Fedorov, N.; Tallapragada, K.; Breining, S. R.; Miller, C. H. Pharmacological properties and predicted binding mode of arylmethylene quinuclidine-like derivatives at the $\alpha3\beta4$ nicotinic acetylcholine receptor (nAChR). *Bioorg. Med. Chem. Lett.* **2013**, *23*, 1450−1455.

(24) Hauser, T. A.; Hepler, C. D.; Kombo, D. C.; Grinevich, V.; Kiser, M. N.; Hooker, D. N.; Zhang, J.; Mountfort, D.; Selwood, A.; Akireddy, S. R.; Letchworth, S. R.; Yohannes, D. Comparison of acetylcholine receptor interactions of the marine toxins, 13-desmethylspirolide C and gymnodimine. *Neuropharmacology* **2012**, *62*, 2238−2249.

(25) Mazurov, A. A.; Kombo, D. C.; Hauser, T. A.; Miao, L.; Dull, G.; Genus, J. F.; Fedorov, N. B.; Benson, L.; Sidach, S.; Xiao, Y.; Hammond, P. S.; James, J. W.; Miller, C. H.; Yohannes, D. Discovery of (2S,3R)-N-[2-(pyridin-3-ylmethyl)-1-azabicyclo[2.2.2]oct-3-yl]-benzo[b]furan-2-carboxamide (TC-5619), a selective $\alpha7$ nicotinic acetylcholine receptor agonist, for the treatment of cognitive disorders. *J. Med. Chem.* **2012**, *55*, 9793−9809.

(26) Mazurov, A. A.; Kombo, D. C.; Akireddy, S.; Murthy, S.; Hauser, T. A.; Jordan, K. J.; Gatto, G. G.; Yohannes, D. Novel nicotinic acetylcholine receptor agonists containing carbonyl moiety as a hydrogen bond acceptor. *Bioorg. Med. Chem. Lett.* **2013**, *23*, 3927-3934.

(27) Mazurov, A. A.; Miao, L.; Bhatti, B. S.; Strachan, J.-P.; Akireddy, S.; Murthy, S.; Kombo, D.; Xiao, Y.-D.; Hammond, P. S.; Zhang, J.; Hauser, T. A.; Jordan, K. G.; Miller, C. H.; Speake, J. D.; Gatto, G. J.; Yohannes, D. Discovery of 3-(5-chloro-2-furoyl)-3,7-diazabicyclo[3.3.0]octane (TC-6683, AZD1446), a novel highly selective $\alpha4\beta2$ nicotinic acetylcholine receptor agonist for the treatment of cognitive disorders. *J. Med. Chem.* **2012**, *55*, 9181−9194.

(28) Kombo, D. C.; Mazurov, A. A.; Strachan, J. P.; Bencherif, M. Computational studies of novel carbonyl-containing diazabicyclic ligands interacting with $\alpha4\beta2$ nicotinic acetylcholine receptor (nAChR) reveal alternative binding modes. *Bioorg. Med. Chem. Lett.* **2013**, *23*, 5105−5113.

(29) Kombo, D. C.; Grinevich, V.; Hauser, T. A.; Sidach, S.; Bencherif, M. QM-polarized ligand docking accurately predicts the trend in binding affinity of a series of arylmethylene quinuclidine-like derivatives at the $\alpha4\beta2$ and $\alpha3\beta4$ nicotinic acetylcholine receptors (nAChRs). *Bioorg. Med. Chem. Lett.* **2013**, *23*, 4842−4847.

(30) Kombo, D. C.; Tallapragada, K.; Jain, R.; Chewning, J.; Mazurov, A. A.; Speake, J. D.; Hauser, T. A.; Toler, S. 3D molecular descriptors important for clinical success. *J. Chem. Inf. Model.* **2013**, *53*, 327−342.

(31) Molgó, J.; Araoz, R.; Benoit, E.; Iorga, B. I. Physical and virtual screening methods for marine toxins and drug discovery targeting nicotinic acetylcholine receptors. *Expert Opin. Drug Discovery*. **2013** Aug 6. [Epub ahead of print].

(32) Chen, S. G.; Gu, R. X.; Dai, H.; Wei, D. Q. Virtual screening for alpha7 nicotinic acetylcholine receptor for treatment of Alzheimer's disease. *J. Mol. Graphics Modell.* **2013**, Feb;39:98-107. doi: 10.1016/j.jmgm.2012.11.008. Epub 2012 Nov 29.
(33) Blum, L. C.; van Deursen, R.; Bertrand, S.; Mayer, M.; Burgi, J. J.; Bertrand, D.; Reymond, J. L. Discovery of α7-nicotinic receptor ligands by virtual screening of the chemical universe database GDB-13. *J. Chem. Inf. Model.* **2011**, *51*, 3105−3112.
(34) Utsintong, M.; Rojsanga, P.; Ho, K. Y.; Talley, T. T.; Olson, A. J.; Matsumoto, K.; Vajragupta, O. Virtual screening against acetylcholine binding protein. *J. Biomol. Screening* **2012**, *17*, 204−215.
(35) Reymond, J. L.; van Deursen, R.; Bertrand, D. What we have learned from crystal structures of proteins to receptor function. *Biochem. Pharmacol.* **2011**, *82*, 1521−1527.
(36) Dey, R.; Chen, L. In search of allosteric modulators of a7-nAChR by solvent density guided virtual screening. *J. Biomol. Struct. Dyn.* **2011**, *28*, 695−715.
(37) Peng, Y.; Zhang, Q.; Snyder, G. L.; Zhu, H.; Yao, W.; Tomesch, J.; Papke, R. L.; O'Callaghan, J. P.; Welsh, W. J.; Wennogle, L. P. Discovery of novel alpha7 nicotinic receptor antagonists. *Bioorg. Med. Chem. Lett.* **2010**, *20*, 4825−4830.
(38) Grazioso, G.; Pome, D. Y.; Matera, C.; Frigerio, F.; Pucci, L.; Gotti, C.; Dallanoce, C.; De Amici, M. Design of novel alpha7-subtype-preferring nicotinic acetylcholine receptor agonists: application of docking and MM-PBSA computational approaches, synthetic and pharmacological studies. *Bioorg. Med. Chem. Lett.* **2009**, *19*, 6353−6357.
(39) Utsintong, M.; Talley, T. T.; Taylor, P. W.; Olson, A. J.; Vajragupta, O. Virtual screening against alpha-cobratoxin. *J. Biomol. Screening* **2009**, *14*, 1109−1118.
(40) Babakhani, A.; Talley, T. T.; Taylor, P. W.; McCammon, J. A. A virtual screening study of the acetylcholine binding protein using a relaxed-complex approach. *Comput. Biol. Chem.* **2009**, *33*, 160−170.
(41) Ulens, C.; Akdemir, A.; Jongejan, A.; van Elk, R.; Bertrand, S.; Perrakis, A.; Leurs, R.; Smit, A. B.; Sixma, T. K.; Bertrand, D.; de Esch, I. J. Use of acetylcholine binding protein in the search for novel alpha7 nicotinic receptor ligands. In silico docking, pharmacological screening, and X-ray analysis. *J. Med. Chem.* **2009**, *52*, 2372−2383.
(42) Quik, M.; Campos, C.; Bordia, T.; Strachan, J. P.; Zhang, J.; McIntosh, J. M.; Letchworth, S.; Jordan, K. α4β2 nicotinic receptors play a role in the nAChR-mediated decline in L-dopa-induced dyskinesias in parkinsonian rats. *Neuropharmacology* **2013**, *71*, 191−203.
(43) Sali, A.; Blundell, T. L. Comparative protein modelling by satisfaction of spatial restraints. *J. Mol. Biol.* **1993**, *234*, 779−815.
(44) Letchworth, S. R.; Whiteaker, P. Progress and challenges in the study of α6-containing nicotinic acetylcholine receptors. *Biochem. Pharmacol.* **2011**, *82*, 862−872.
(45) Young, T.; Abel, R.; Kim, B.; Berne, B. J.; Friesner, R. A. Motifs for molecular recognition exploiting hydrophobic enclosure in protein-ligand binding. *Proc. Natl. Acad. Sci. U. S. A.* **2007**, *104*, 808−813.
(46) Friesner, R. A.; Murphy, R. B.; Repasky, M. P.; Frye, L. L.; Greenwood, J. R.; Halgren, T. A.; Sanschagrin, P. C.; Mainz, D. T. Extra precision glide: docking and scoring incorporating a model of hydrophobic enclosure for protein-ligand complexes. *J. Med. Chem.* **2006**, *49*, 6177−6196.
(47) Strachan, J. P.; Cuthbertson, T.; Wirth, D. D.; Dull, G. M.; Letchworth, S. R.; Jordan, K. G.; Kombo, D. C. Targacept, Inc. Publication date: September 2012. PCT/US2012/028691.
(48) Kucinski, A.; Wersinger, S.; Stachowiak, E. K.; Corso, T. D.; Parry, M. J.; Zhang, J.; Jordan, K.; Letchworth, S.; Bencherif, M.; Stachowiak, M. K. Neuronal nicotinic receptor agonists ameliorate spontaneous motor asymmetries and motor discoordination in a unilateral mouse model of Parkinson's Disease. *Pharm. Biochem. Behav.* **2013**, Jul 16. pii: S0091-3057(13)00173-1. doi: 10.1016/j.pbb.2013.07.005. [Epub ahead of print].
(49) Xiu, X.; Puskar, N. L.; Shanata, J. A.; Lester, H. A.; Dougherty, D. A. Nicotine binding to brain receptors requires a strong cation-pi interaction. *Nature* **2009**, *458*, 534−537.
(50) Xiao, Y.; Hammond, P.; Mazurov, A. A.; Yohannes, D. Multiple interaction regions in the orthosteric ligand binding domain of the α7 neuronal nicotinic acetylcholine receptor. *J. Chem. Inf. Model.* **2012**, *52*, 3064−3073.